Influence of the anion in tin-based EUV photoresists properties

Quentin Evrard*[1], Najmeh Sadegh[5], Chao Chun Hsu[1], Nicola Mahne[2], Angelo Giglia[2], Stefano Nannarone[2] Yasin Ekinci[3], Michaela Vockenhuber[3], Akira Nishimura[4], Tsuyoshi Goya[4], Takuo Sugioka[4] and Albert M. Brouwer[1]

[1] Van't Hoff Institute for Molecular Sciences, University of Amsterdam, P.O. Box 94157, 1090 GD Amsterdam, The Netherlands; [2] CNR-IOM, Strada Statale 14 km 163,5 - 34149 Basovizza – Trieste, Italy; [3] Paul Scherrer Institute, Forschungsstrasse 111, 5232 Villigen PSI, Switzerland; [4] Nippon Shokubai, 5-8 Nishi Otabi-cho, Suita, Osaka, 564-0034, Japan; [5] ARCNL, Science Park 106, 1098 XG Amsterdam, The Netherlands

*q.j.o.evrard@uva.nl

ABSTRACT

In this work we assess the effect of the change of counter-anions on the photolithography properties of butyl-Sn_{12} oxo hydroxo cages. The hydroxide anions were exchanged with tetrakis(pentafluorophenyl)borate $(B(PFP)_4)^-$ and (phenyl) trifluoroborate $(BF_3Ph)^-$ anions which exhibit a photoabsorption cross section at 92 eV that is similar to that of the butyl-Sn_{12} oxo hydroxo cages. The degradation of the EUV photoresist was monitored via in-situ EUV exposure followed by X-ray photoelectron spectroscopy (XPS) at the BEAR beamline (Elettra, Italy) at the C1s-edge. Both systems exhibit similar carbon losses of around 25% for 100 mJ/cm^2 dose. The Sn_{12} cluster with acetate anions, as a reference compound, exhibit a loss of C1s XPS signal from the butyl chains of around 23% for the same 100 mJ/cm^2 EUV exposure dose indicating a larger degradation of the Sn_{12} cluster for the latter. We also evaluated the patterning performance of the $Sn_{12}(B(PFP)_4)$ resist via interference lithography at the XIL-II beamline (PSI, Switzerland) and found the positive tone character of the resist and its ability to write lines with 50 nm half pitch resolution for doses of 30 mJ/cm^2. In contrast, $Sn_{12}(BF_3Ph)$ acts as a sensitive negative tone resist, with doses of 12.5 mJ/cm^2 sufficient to write 50 nm half pitch lines.

Keywords: EUV lithography, Tin based photoresist, Tin-oxo-hydroxo cage, Inorganic-organic hybrid photoresist

1. INTRODUCTION

Extreme ultraviolet (EUV) lithography is the cornerstone of all advanced photolithography processes progressively bound to replace multipatterning immersion argon fluoride processes[1]. The use for EUV of organic resists traditionally employed for ArF lithography poses a significant challenge due to a combination of the ionizing character of EUV radiation, the fundamental difference in reaction pathways and the harsher requirement for etch resistance[2]. The need for newly designed EUV photoresists has led to intense investigation of inorganic molecular materials[3,4]. Among these materials tin oxo hydroxo cages[5] are very promising photoresists. The tin oxo cages presented in this work are positively charged clusters of twelve tin atoms bridged by oxygen and have one butyl group attached to each tin atom forming a layer at the surface of the inorganic core enhancing its solubility (see figure 1). The tin-carbon bonds can be cleaved upon EUV exposure[6,7]. Models suggest[8] that this dissociation is generating active sites on the tin atoms that lead to the cross-linking between neighbouring clusters, rendering the material insoluble. The detailed molecular-level chemical changes that give rise to the solubility switch are as yet unknown.
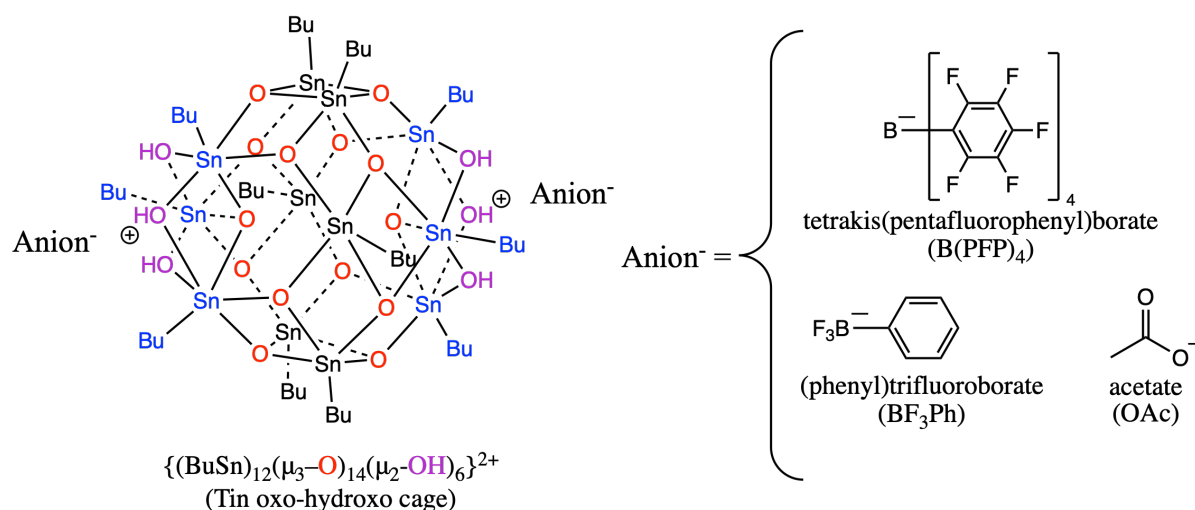
Figure 1. Structure of butyl-Sn_{12} oxo hydroxo cages and anions used in this work

The present work mainly focuses on the effect of the change of counteranion on their EUV and lithographic properties, indeed, tin oxo cages are well known for their anion exchange capabilities[9]. One target for these resists is to further increase their EUV absorption cross-section to generate more active sites and to increase the photoresist sensitivity. To that end we exchange the hydroxide anions typically present on the tin oxo cages with fluorinated counteranions having higher EUV absorption cross-section such as tetrakis(pentafluorophenyl)borate (B(PFP)$_4$) or (phenyl)trifluoroborate (BF$_3$Ph). Surprisingly, changing counterions considerably affects the patterning behaviour.

2. EXPERIMENT

2.1 Thin film sample preparation

The photoresist solution of **Tin(B(PFP)$_4$)$_2$** (10 mg/mL) or **Tin(BF$_3$Ph)$_2$** (10 mg/mL) are prepared in trifluorotoluene and sonicated for 10 minutes. All the solutions are then filtered using a 0.20 μm PTFE filter and spincoated directly. For **Tin(OAc)$_2$** the solution (10mg/mL) is prepared with the same protocol but with toluene as a spin coating solvent. The photoresist solutions of all samples for EUV lithography were prepared on silicon wafers (Siegert Wafer, CZ growth, p-type B-doped, <100>, resistivity 5-10 Ohm-cm) used without further cleaning. The spin coating is done with a rotation speed of 2000 rpm, an acceleration of 750 rpm/s and no post-application or post-exposure baking are performed. The thickness of the obtained films using this procedure is 30-35 nm.

The **Tin(B(PFP)$_4$)$_2$** and **Tin(OAc)$_2$** samples for in-situ EUV exposures with XPS spectroscopy were prepared on gold-coated Si substrates, while the thin film of **Tin(BF$_3$Ph)$_2$** was prepared on bare silicon. The silicon wafer (Siegert Wafer, CZ growth, p-type B-doped, <100>, resistivity 5-10 Ohm-cm) is first diced in 25 × 25 mm substrates. The substrates are cleaned with an 80°C base piranha solution for 15 minutes, rinsed with isopropanol and dried with nitrogen flow. They are then cleaned using an ozone plasma (Diener Electronic Pico QR-200-PCCE) with a two-minute oxygen plasma at 0.2 mbar working pressure. Next, the samples are coated with a gold layer using a sputter coater (Leica EM ACE600 double sputter coater) depositing a 5 nm layer of chromium as adhesion layer followed by 30 nm of gold. The gold-coated substrates are used for spin-coating of the resist solutions, with a rotation speed of 2500 rpm and an acceleration of 750 rpm/s. No pre- or post-exposure baking is performed.

2.2 Measurement setup

The Atomic Force Microscopy measurements are performed on a Bruker Dimension Icon using tapping mode with Bruker TESP-SS tips (320 kHz, 42 N/m), fields of 3×0.6 µm were measured with 256 samples per line and a scanning frequency of 0.6 Hz. Raw data was corrected by truncated mean method and flattened by mean plane. No further corrections were made.

The XPS spectra have been collected at the IOM-CNR BEAR beamline (Elettra synchrotron, Trieste, Italy) using a hemispherical deflection electron analyzer (66 mm mean radius) driven at constant pass energy. Spectra were collected at normal emission with the beam hitting the sample at 45° with respect to the surface normal angle. The sample of interest is first exposed to 92 eV (EUV) irradiation of the desired dose, then XPS is performed with an incident energy of 400 eV for carbon 1s edge with triplicate measurements on freshly exposed spots to increase the signal-to-noise. Because of the sensitivity of the material, extra care has been taken to minimize the spectra acquisition time.

3. RESULTS

3.1 In-situ EUV exposure and X-ray photoelectron spectroscopy

The samples were prepared as described in section 2.2 on gold substrate to mitigate charging effects. All measurements are done in triplicate on different sample position and averaged to increase the signal/noise ratio. The XPS data was recorded for sample **Tin(B(PFP)₄)₂** as well as **Tin(BF₃Ph)₂**, and **Tin(OAc)₂** was added as a reference sample and a model in terms of top performer[10] in terms of sensitivity. The reference spectra collected for **Tin(OAc)₂** (figure 2) show the expected signal loss for Sn_{12} clusters. Indeed, the signal coming from the butyl chains at 286 eV is progressively reduced by EUV exposure as the Sn-C bonds are broken and the butyl chains are lost by outgassing in the high vacuum of the experimental chamber. A loss of 23% of the carbon signal is observed at 100 mJ/cm^2 EUV dose and further exposure leads to a loss of 39% at a dose of 500 mJ/cm^2 (Figure 3).
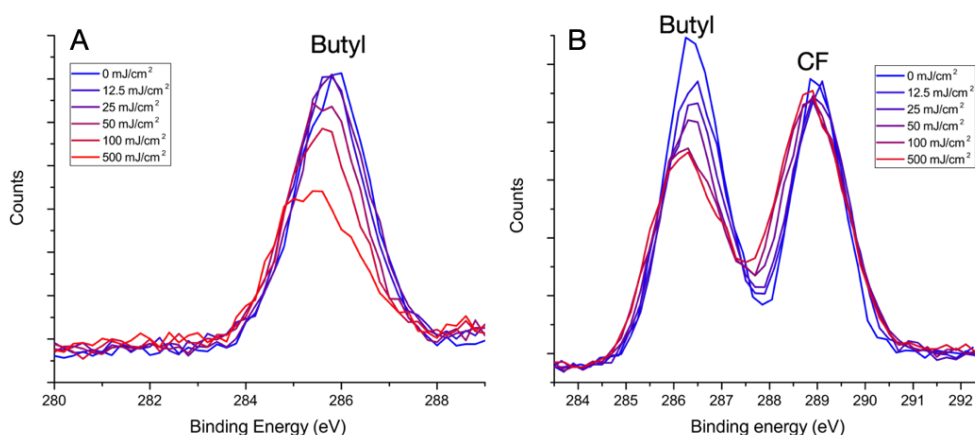

Figure 2. X-ray photoelectron spectra of the C1s edge of **Tin(OAc)₂** (A) and **Tin(B(PFP)₄)₂** (B) after 92 eV exposure, the signal at 289 eV binding energy on the left stems from the B(PFP)₄ anion.

For **Tin(B(PFP)₄)₂** two different peaks can be observed at 286.5 and 289 eV. The peak at 289 eV binding energy corresponds to the carbon atoms present in the anion and bound to the fluorine and it appears to be unaffected by the EUV exposure. The peak at a binding energy of 286.5 eV corresponds to the butyl chains of the Sn_{12} cluster. In this case a 22% loss is observed at 100 mJ/cm^2 EUV dose which is similar to the **Tin(OAc)₂** however a plateau is being reached above 100 mJ/cm^2 as a decrease of only 27% is observed at 500 mJ/cm^2 as opposed to the 39% of the **Tin(OAc)₂** reference compound (figure 3A). A shift of around 0.5 eV towards lower binding energies is observed in all spectra that have been exposed to high EUV doses; this shift could be due to the change in the work function of the material due to its degradation.
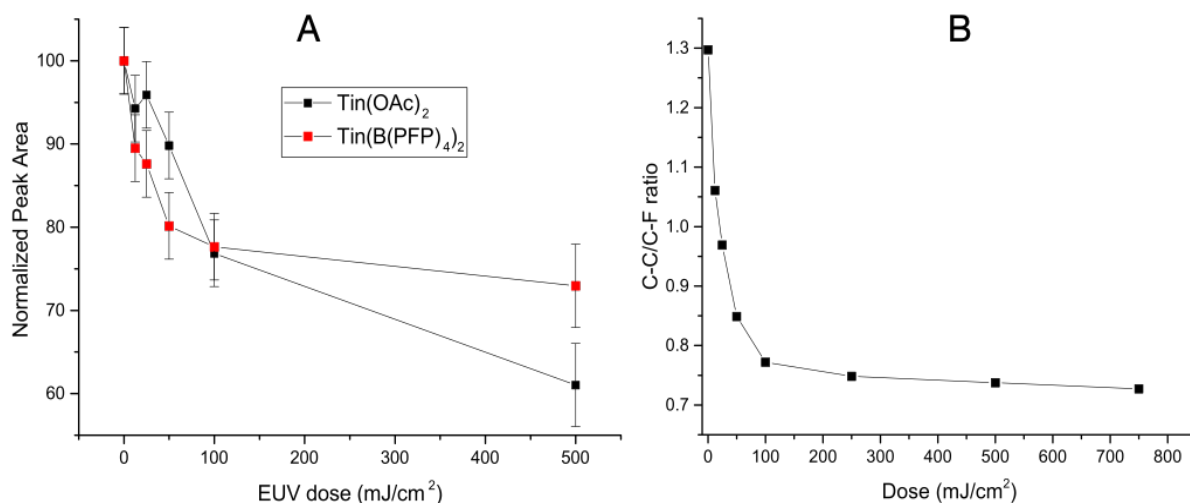
Figure 3. Normalized XPS peak intensities of butyl chains for **Tin(OAc)₂** and **Tin(B(PFP)₄)₂** (A) and ratio of XPS signal of butyl chains over B(PFP)₄ anion of **Tin(B(PFP)₄)₂** (B).

The ratio of peak areas stemming from the butyl chains from the Sn_{12} cluster and the $B(PFP)_4$ anion for the unexposed material (theoretical value 1.4) decreases to 0.75 for exposed material, and changes only slowly after a dose of 100 mJ/cm^2 further emphasizing the lower conversion increase at higher doses. In previous work, we have presented the EUV reactivity of **Tin(B(PFP)₄)₂** and compared it with that of compounds with large tetraphenylborate anions[11]. Here we extend the study in a different direction, and consider BF_3-aryl anions, represented by its simplest example phenyltrifluoroborate $PhBF_3^-$. Results of in situ EUV/XPS experiments on **Tin(BF₃Ph)₂** (figure 4) exhibit similar carbon losses as **Tin(B(PFP)₄)₂** and the reference compound with a ~25% loss observed for 100 mJ/cm^2 EUV exposure dose.
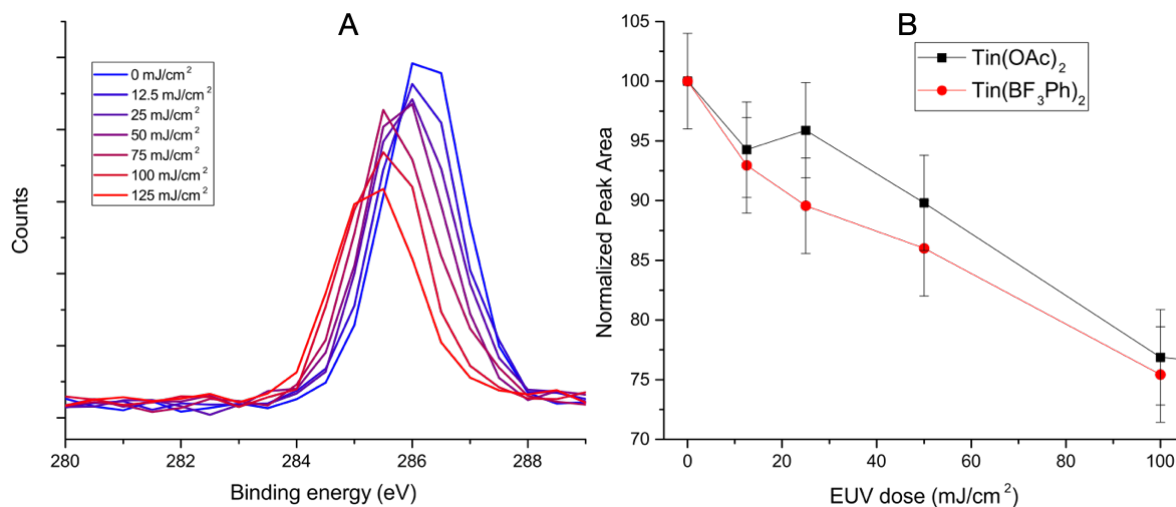

Figure 4. X-ray photoelectron spectra of the C1s edge of **Tin(BF₃Ph)₂** (A) and normalized XPS peak intensities of butyl chains for **Tin(OAc)₂** and **Tin(BF₃Ph)₂** (B).

The XPS data for **Tin(BF₃Ph)₂** shows a peak at 286 eV binding energy and is due mainly to the butyl chains of the Sn_{12} cluster. The aromatic carbons in the BF_3Ph have a similar binding energy, and both signals are present in the same peak. The overall carbon bleaching is slightly faster in the 0-100 mJ/cm^2 dose range for **Tin(B(PFP)₄)₂** and **Tin(BF₃Ph)₂** compared to **Tin(OAc)₂** but as shown in the next section, their sensitivity and patterning properties differ considerably.

3.2 EUV interference lithography

The performance of **Tin(B(PFP)$_4$)$_2$** has been studied at the Paul Scherrer Institute (Switzerland) on the XIL-II beamline via interference lithography producing line/space patterns on the resist. The samples were prepared as described in section 2.1. In figure 5 we compare the effect of two developers on the obtained pattern that has been monitored via atomic force microscopy (AFM) imaging.
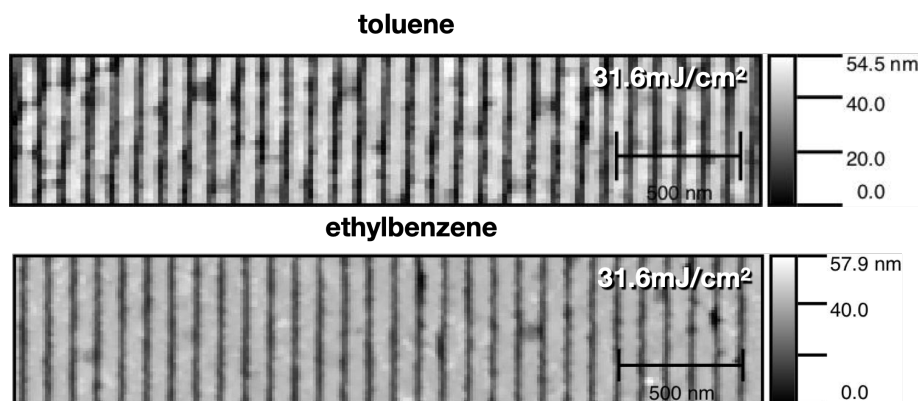

Figure 5. AFM height images obtained from **Tin(B(PFP)$_4$)$_2$** exposed to EUV irradiation (Line-space patterns with 50 nm half-pitch) and then developed with toluene (top) and ethylbenzene (bottom).

Using toluene as developer for **Tin(B(PFP)$_4$)$_2$** surprisingly led to the formation of a positive tone pattern of 50 nm half pitch from around 30 mJ/cm^2 up to 100 mJ/cm^2 EUV dose. Toluene, however, proved to be too aggressive as a developer leading to cracks and other defects in the obtained pattern. To mitigate these issues ethylbenzene was used instead and this led to the improved pattern (figure 5, bottom). This minor change in developer led to a decrease in overall film defects while keeping the same range of EUV dose of 30-100 mJ/cm^2 needed to retain the positive tone pattern.

The overall pattern quality, however, needs improvement and writing smaller patterns (down to 22 nm HP) required 50 mJ/cm^2 to clear, and dramatically increased pattern defects with lift off or cracks. Further work is required to decrease film defects that are revealed by the development process.

The second compound analyzed, **Tin(BF$_3$Ph)$_2$**, has been studied in the same conditions as **Tin(B(PFP)$_4$)$_2$** except that the developer used was light petroleum ether (40-60). The patterning results shown in the figure 6 below indicate a better sensitivity of the material as well as a noticeable increase in the pattern quality.
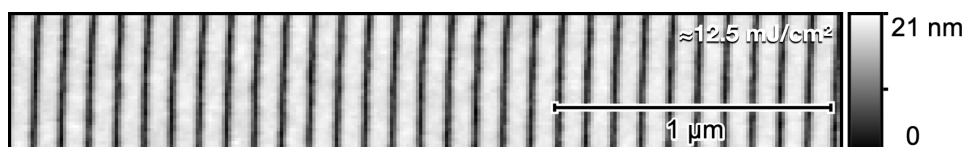

Figure 6. AFM height images obtained from **Tin(BF$_3$Ph)$_2$** exposed to EUV irradiation (Line-space patterns with 50 nm half-pitch) and developed with light petroleum ether.

Among these differences the pattern is also negative tone instead of positive which is more in line with the commonly observed Sn$_{12}$-based EUV photoresist properties. As the EUV absorption is similar for all of the studied systems the interactions between the anions and Sn$_{12}$ cage upon EUV exposure has to be considered when comparing the drastic differences in both sensitivity and solubility switch mechanics.

4. CONCLUSIONS

In the present work, we synthesized new Sn_{12} cluster based photoresist **Tin(B(PFP)₄)₂** and **Tin(BF₃Ph)₂** compounds via anion exchange, demonstrated the ability to form thin films of 30-40 nm of the materials by using trifluorotoluene as spincoating solvent. The in situ XPS measurements of both photoresist shows a bleaching of its butyl chains at a similar rate compared to reference material **Tin(OAc)₂** but reaching a plateau at doses higher than 100 mJ/cm² of EUV dose exposure for **Tin(B(PFP)₄)₂**. The **Tin(B(PFP)₄)₂** compound performance in EUV photolithography has also been assessed and surprisingly the resist was found to be a positive tone photoresist as opposed to other Sn_{12} cluster based photoresist studied so far. The patterning performance of **Tin(BF₃Ph)₂** is significantly superior both in sensitivity and pattern quality compared to **Tin(B(PFP)₄)₂**, however **Tin(BF₃Ph)₂** is a negative tone photoresist, the significant differences in solubility switch from both systems must stem from anion-Sn_{12} cage interactions upon EUV exposure.

REFERENCES

[1] Wagner, C. and Harned, N., "Lithography gets extreme", Nat. Photon. 4, 24-26 (2010).

[2] Trikeriotis, M., Jin Bae, W., Schwartz, E., Krysak, M., Lafferty, N., Xie, P., Smith, B., Zimmerman, P. A., Ober, C. K., Giannelis, E. P., " Development of an inorganic photoresist for DUV, EUV, and electron beam imaging", Proc. SPIE 7639, (2010)

[3] Krysak, M., Blackwell, J., Putna, S., Leeson, M., Younkin, T., Harlson, S., Frasure, K., Gstrein, F. "Investigation of novel inorganic resist materials for EUV lithography", Proc. SPIE 9048, (2014)

[4] Wang, Z., Yao, X., An, H., Wang, Y., Chen, J., Wang, S., Guo, X., Yu, T., Zeng, Y., Yang, G. Li, Y. "Recent Advances in Organic-inorganic Hybrid Photoresists", J. Microelectron. Manuf. 4, 1-8 (2021).

[5] Cardineau, B., Del Re, R., Marnell, M., Al-Mashat, H., Vockenhuber, M., Ekinci, Y., Sarma, C. Freedman, D. A., Brainard, R. L. "Photolithographic properties of tin-oxo clusters using extreme ultraviolet light (13.5nm)." Microelectron. Eng. 127, 44-50 (2014).

[6] Haitjema, J., Wu, L., Giuliani, A., Nahon, L., Castellanos, S., Brouwer, A. M. "UV and VUV-induced fragmentation of tin-oxo cage ions.", Phys. Chem. Chem. Phys. 23, 20909-20918 (2021).

[7] Haitjema, J., Wu, L., Giuliani, A., Nahon, L., Castellanos, S., Brouwer, A. M. "Photo-induced Fragmentation of a Tin-oxo Cage Compound." J. Photopolym. Sci. Technol. 31, 243-247 (2018).

[8] Hinsberg, W. D. & Meyers, S. "A numeric model for the imaging mechanism of metal oxide EUV resists.", Proc. SPIE 10146, (2017).

[9] Eychenne-Baron, C., Ribot, F., Sanchez, C. "New synthesis of the nanobuilding block $\{(BuSn)_{12}O_{14}(OH)_6\}^{2+}$ and exchange properties of $\{(BuSn)_{12}O_{14}(OH)_6\}(O_3SC_6H_4CH_3)_2$". J. Organomet. Chem. 567, 137-142 (1998).

[10] Haitjema, J., Zhang, Y., Vockenhuber, M., Kazazis, D., Ekinci, Y., Brouwer, A. M., "Extreme ultraviolet patterning of tin-oxo cages.", J. Micro/Nanolith., MEMS MOEMS 16, 033510 (2017).

[11] Evrard, Q., Sadegh, N., Ekinci, Y. Vockenhuber, M., Mahne, N., Giglia, A., Nannarone, S., Goya, T. Sugioka, T., Brouwer, A.M. "Influence of counteranions on the performance of tin-based EUV photoresists" J. Photopolym. Sci. Tech., 35 (2022). In press.